Journal of Power Sources 188 (2009) 338–342

Contents lists available at ScienceDirect

Journal of Power Sources

journal homepage: www.elsevier.com/locate/jpowsour

Short communication

Characterization of honeycomb-like "β-Ni(OH)$_2$" thin films synthesized by chemical bath deposition method and their supercapacitor application

U.M. Patil [a], K.V. Gurav [a], V.J. Fulari [a], C.D. Lokhande [a,b,*], Oh Shim Joo [b,**]

[a] Thin Film Physics Laboratory, Department of Physics, Shivaji University, Kolhapur 416 004 (M.S.), India
[b] Clean Energy Research Center, Korea Institute of Science and Technology, P.O. Box 131, Cheongryang, Seoul 130-650, Republic of Korea

ARTICLE INFO

Article history:
Received 25 July 2008
Received in revised form 28 October 2008
Accepted 5 November 2008
Available online 13 December 2008

Keywords:
Nickel hydroxide thin film
Chemical bath deposition
Optical properties
Electrical properties
Surface morphology
Supercapacitor behaviour

ABSTRACT

Nanostructured nickel hydroxide thin films are synthesized via a simple chemical bath deposition (CBD) method using nickel nitrate Ni(NO$_3$)$_2$ as the starting material. The deposition process is based on the thermal decomposition of ammonia-complexed nickel ions at 333 K. The structural, surface morphological, optical, electrical and electrochemical properties of the films are examined. The nanocrystalline "β" phase of Ni(OH)$_2$ is confirmed by the X-ray diffraction analysis. Scanning electron microscopy reveals a macroporous and interconnected honeycomb-like morphology. Optical absorption studies show that "β-Ni(OH)$_2$" has a wide optical band-gap of 3.95 eV. The negative temperature coefficient of the electrical resistance of "β-Ni(OH)$_2$", is attributed to the semiconducting nature of the material. The electrochemical properties of "β-Ni(OH)$_2$" in KOH electrolyte are examined by cyclic voltammetric (CV) measurements. The scan-rate dependent voltammograms demonstrate pseudocapacitive behaviour when "β-Ni(OH)$_2$" is employed as a working electrode in a three-electrode electrochemical cell containing 2 M KOH electrolyte with a platinum counter electrode and a saturated calomel reference electrodes. A specific capacitance of ~398 × 10^3 F kg^{-1} is obtained.

1. Introduction

Nickel hydroxide exists in a variety of forms. Four polymorphs of nickel hydroxide are observed over the lifetime of the nickel electrode, namely: α-Ni(OH)$_2$, β-Ni(OH)$_2$, β-NiOOH and γ-NiOOH [1–3]. The two most common forms are the α and β polymorphs α-Ni(OH)$_2$ consists of stacked Ni(OH)$_{2-x}$ layers intercalated with various anions or water molecules and is isostructural with hydrotalcite-like compounds. Anhydrous β-Ni(OH)$_2$ does not have intercalated species has a brucite-like structure [4–6]. These various forms of nickel hydroxide differ from each other in their chemical structure, degree of hydration and morphology [5].

Nickel hydroxide compounds attract a wide interest in technical and industrial applications. Nickel hydroxide is the positive electrode material of all the nickel-based secondary batteries, including Ni–Cd, Ni–Fe, Ni–Zn, Ni–H$_2$ and Ni–MH (metal hydride). These rechargeable alkaline batteries are usually positive-limited, so that the capacity and cycle-life of the cells are determined mainly by the properties of nickel hydroxide active materials and the corresponding electrodes [1–5]. The practical importance of the nickel hydroxide structure and its electrochemical properties applies not only to batteries applications, but also to fuel cells, electrochemical capacitors, electrolyzers, electrosynthetic cells, solar cells and electrochromic devices [6–9]. Nickel hydroxide is an important material because of the relative ease with which it is transformed into other materials. Nickel oxides, which can be obtained through the heating of nickel hydroxide, are industrially used in catalysis [10,11]. Nickel hydroxide is also employed as an additive in lubricants and has been shown to provide good anti-corrosion properties to surfaces [12].

Nickel hydroxide is a promising candidate for crystal size reduction, yielding better electrochemical properties, according to Watanabe et al. [13]. If electrodes in nickel systems could be coated with nickel hydroxide nanoparticles easily and reliably, then lower-cost battery systems could be created with increased specific energy and larger capacities. Furthermore, coatings of nanoparticles of nickel hydroxide would be of interest in catalytic applications [10–12]. As discussed above, in order to improve the electrochemical activity and charge–discharge performance of nickel hydroxide materials, the trend is to reduce the crystallite size, increase the structural defects and enhance the specific surface area. Such objectives have led to the development of nanostructured nickel hydroxides.

The chemical methods involve simple processes and are easy to control. Various chemical methods have been used to prepare nanostructure nickel hydroxide, namely, common chemical precip-

* Corresponding author at: Thin Film Physics Laboratory, Department of Physics, Shivaji University, Kolhapur 416 004 (M.S.), India. Tel.: +91 0231 2609229.
** Corresponding author.
E-mail addresses: l.chandrakant@yahoo.com (C.D. Lokhande), joocat@kist.re.kr (O.S. Joo).

0378-7753/$ – see front matter © 2009 Published by Elsevier B.V.
doi:10.1016/j.jpowsour.2008.11.136

itation [14], sol–gel synthesis [15], urea homogeneous precipitation [16], electrochemical deposition [17], and chemical bath deposition (CBD) [18–20]. The CBD method is presently attracting considerable attention, as it does not require sophisticated instrumentation; any insoluble surface to which the solution has a free access will be a suitable substrate for the deposition. The low-temperature deposition avoids oxidation and corrosion of metallic substrates. The CBD procedure results in pinhole-free and uniform deposits since the basic building blocks are ions instead of atoms [21,22].

The present investigation, reports the synthesis of a novel, nanocrystalline, honeycomb-structured, nickel hydroxide electrode by a low-temperature CBD method. The structural, surface morphological, optical, electrical and electrochemical capacitive properties of the electrode are evaluated.

2. Experimental

Preparation of nickel hydroxide thin films by the CBD method is based on the heating of an alkaline bath of nickel nitrate that contains the substrates. The alkaline bath was prepared from 0.1 M $Ni(NO_3)_2{\cdot}6H_2O$ as a source of nickel and aqueous ammonia. The initial precipitate of nickel hydroxide was dissolved after further addition of aqueous ammonia. The pH of the resultant solution was ~12. Glass microslides and stainless steel were used as the substrates, which were successively cleaned with detergent and chromic acid, reused with double-distilled water and, finally, treated with ultrasonic waves for 900 s. The substrates were immersed in the bath, which was then heated. When the bath attained a temperature of 333 K, precipitation (greenish in colour) commenced. During precipitation, a heterogeneous reaction occurred and nickel hydroxide was deposited on the substrate.

The thickness of the nickel hydroxide film was measured by the weight difference method using a sensitive microbalance. Structural identification of nickel hydroxide films was carried out with a X-ray diffractometer (XRD) [copper target (λ = 1.54056 Å)]. The optical absorption study was carried out within a wavelength of range 300–800 ($\times 10^{-9}$ m) using a Systronics Spectrophotometer-119, with glass substrate as reference. The microstructures of films were examined with a scanning electron microscope (SEM) (JEOL-JAPAN 6360). Electrochemical analysis of the films deposited on steel substrates was studied by cyclic voltammetry (CV) using a potentiostat (263A EG&G, Princeton Applied Research Potentiostat). The electrochemical cell comprises a platinum counter electrode, a saturated calomel a reference electrode (SCE) and a β-$Ni(OH)_2$ working electrode immersed in 2 M KOH electrolyte. All potentials are reported with respect to the SCE.

3. Results and discussion

3.1. Film formation mechanism

In the CBD method, film formation is observed when the solution is saturated. The ionic product of anions and cations is equal to the solubility product of the metal hydroxide and when the latter is exceeded, precipitation occurs and ions combine on the substrate and in the solution to form nuclei. Film growth can take place by ion-by-ion condensation of materials or by adsorption of colloidal particles from the solution on the substrate. Formation of a solid phase from a solution involves two steps, namely, nucleation and particle growth. Nucleation is necessary for precipitate formation. The concept of nucleation in solution is that clusters of molecules undergo rapid decomposition and particles combine to grow to a certain film thickness [21].

Generally, metal ions are complexed in such a way that reaction takes place between slowly released metal ions to produce a thin film. Nickel hydroxide thin films have been deposited on glass microslides/steel substrates by slow hydrolysis of nickel nitrate solution. This can be represented by:

$$Ni(NO_3)_2 + 2NH_4OH \rightarrow Ni(OH)_2 + 2NH_4NO_3 \quad (A.1)$$

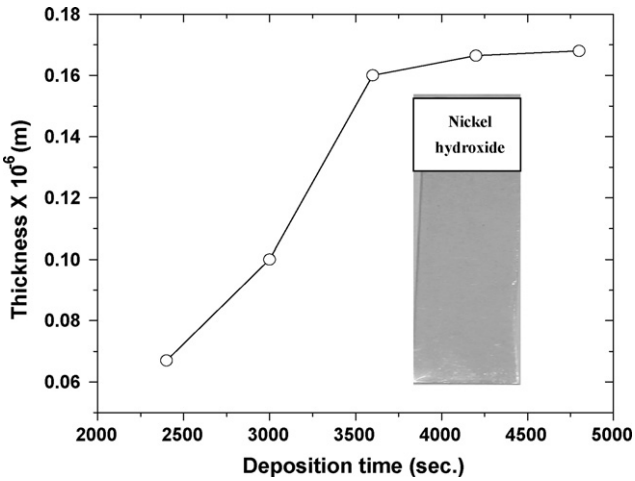

Fig. 1. Variation of nickel hydroxide film thickness as function of deposition time. (Inset: photograph of nickel hydroxide film.)

Variation in the thickness of nickel hydroxide thin films as a function of deposition time is shown in Fig. 4. The film thickness was determined gravimetrically by measuring the change in the weight of the substrate before and after the film deposition and using the bulk density of nickel hydroxide (0.415 kg m^{-3}). The film thickness of nickel hydroxide increases with deposition time, reaches a maximum value (0.17×10^{-6} m) at 4800 s, and then remains constant. Such behaviour can be understood in terms of film formation and continuous precipitation in the bulk of solution [23]. The inset of Fig. 1 is a photograph of the nickel hydroxide thin film, which confirms the feasibility of the CBD method for large area deposition.

3.2. Structural analysis

The X-ray diffractogram of a nickel hydroxide film deposited on a glass substrate is given in Fig. 2. The observed interplaner distance '*d*' values match well with standard [JCPDS card no. 01-1047] '*d*' values and thereby confirm the formation of the "β-$Ni(OH)_2$" compound. Varkey and Fort [18] reported the as-prepared phase of NiOOH from a bath containing 0.1 M-nickel sulfate and ammonia.

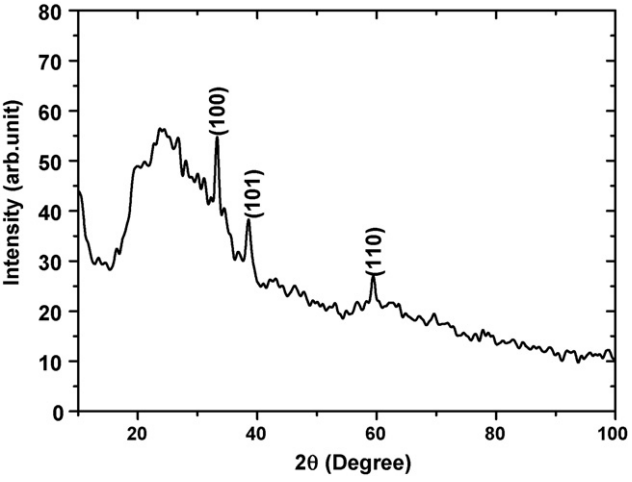

Fig. 2. X-ray diffraction pattern of β-$Ni(OH)_2$ thin film on glass substrate.

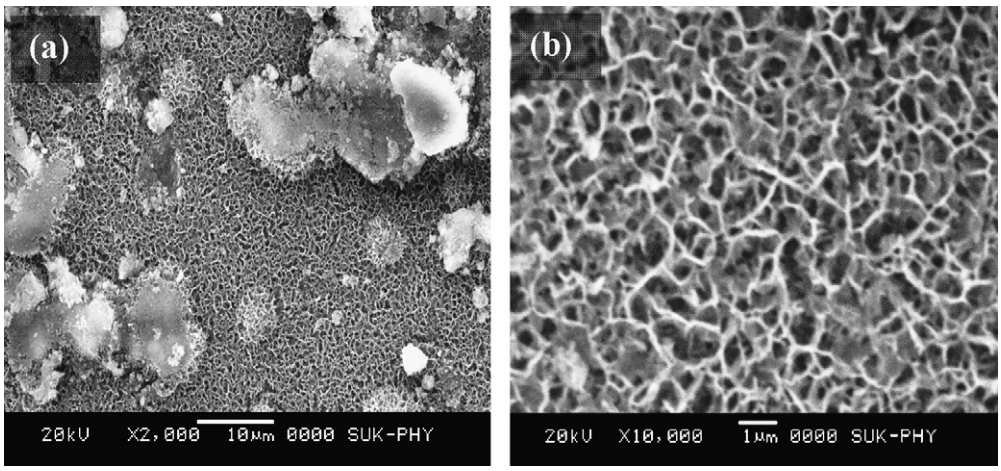

Fig. 3. SEM image of β-Ni(OH)$_2$ thin film at (a) 2000 and (b) 10,000 magnifications.

Berkat et al. [20] produced an as-prepared phase of $3Ni(OH)_2 \cdot 2H_2O$ from a bath containing urea and nickel nitrate. The particle size of the nickel hydroxide thin film is calculated using the Scherrer's relation (with the constant = 0.9) for the (1 0 0) oriented plane. The particle size is found to be about 24 nm.

3.3. Surface morphological studies

SEM micrographs of a "β-Ni(OH)$_2$" thin film deposited on a glass substrate at different magnifications are presented in Fig. 3. The morphology of β-Ni(OH)$_2$ at 2000× magnification if shown in Fig. 3(a). The film is porous and well covered with overgrown particles on the substrate. This overgrowth can be attributed to a nucleation and coalescence process. The surface morphology at 10,000× magnification [Fig. 3(b)] is seen to be a well-covered, interconnected, macroporous; honeycomb-like structure. The flake, nanoparticles and nanorod-like morphologies lead to a high specific surface area and porous volume, which provide the structural foundation for the high specific capacitance [24–27].

3.4. Optical studies

Fig. 4(a) shows the variation of optical absorbance (αt) for a β-Ni(OH)$_2$ thin film with wavelength (λ). The spectrum reveals that film has low absorbance in the visible region of the solar spectrum. Initially, a quick inclining trend in the spectrum is observed. The sharp increase in the absorption at a wavelength of around 330 nm is attributed to the higher band gap of "β-Ni(OH)$_2$". The optical transition type and the band gap, E_g, can be determined from the following relationship.

$$\alpha = \frac{A(E_g - h\nu)^n}{h\nu} \quad \text{(B.1)}$$

where A is a constant, and n is a number equal to 1/2 for a direct-gap and 2 for an indirect-gap compound. The inset of Fig. 4 presents a plot of $(\alpha h\nu)^2$ against $h\nu$ for the"β-Ni(OH)$_2$" film. The relation between $(\alpha h\nu)^2$ versus $h\nu$ implies the direct transition nature for β-Ni(OH)$_2$ films. The band gap, calculated by extrapolating the linear part of the curve to zero absorption ($\alpha = 0$), for the β-Ni(OH)$_2$ film is 3.95 eV. The optical study shows that the β-Ni(OH)$_2$ is a wide-band gap material, which is useful in dye-sensitized solar cells [9]. Varkey and Fort reported the optical gap of 3.76 eV for NiOOH phase [18]. The high optical band-gap of the"β-Ni(OH)$_2$" film may be due to the nanocrystalline nature and the formation of a hydroxide phase.

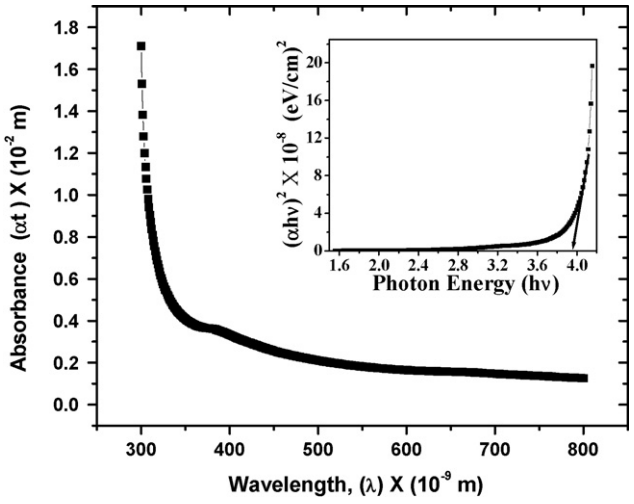

Fig. 4. Variation of absorption (αt) with wavelength (λ) of β-Ni(OH)$_2$ thin film on glass substrate. Inset shows plot of '$(\alpha h\nu)^2$' vs. '$h\nu$' of β-Ni(OH)$_2$ thin film.

3.5. Electrical resistivity

The two-point d.c. probe method was employed to understand the variation of electrical resistivity with temperature of "β-Ni(OH)$_2$" films. The variation of log(ρ) with the reciprocal of temperature (1000/T) is depicted in Fig. 5. It is clearly seen that the "β-Ni(OH)$_2$" film has a negative temperature coefficient of resistance. The room temperature electrical resistivity is of the order of $10^7\ \Omega$ m. The activation energy was calculated using the relation.

$$\rho = \rho_0 \exp(Ea/KT) \quad \text{(C.1)}$$

where ρ is the resistivity at temperature T, ρ_0 is a constant, K is the Boltzmann constant, and Ea is the activation energy. The activation energy is 0.35 eV in the temperature regime, 300–500 K.

3.6. Supercapacitive studies

To evaluate possible application in electrochemical capacitors, the supercapacitor properties of β-Ni(OH)$_2$ electrode were studied by means of CV curves. Fig. 6 shows a typical CV of a β-Ni(OH)$_2$ thin film electrode in 2 M KOH solution at a scan rate 20 mV s^{-1} in the potential range −1 to 1 V. The shape of the CV indicates that the capacitance characteristic is different from that of a electric double-layer capacitance in which the shape is normally close to an ideal

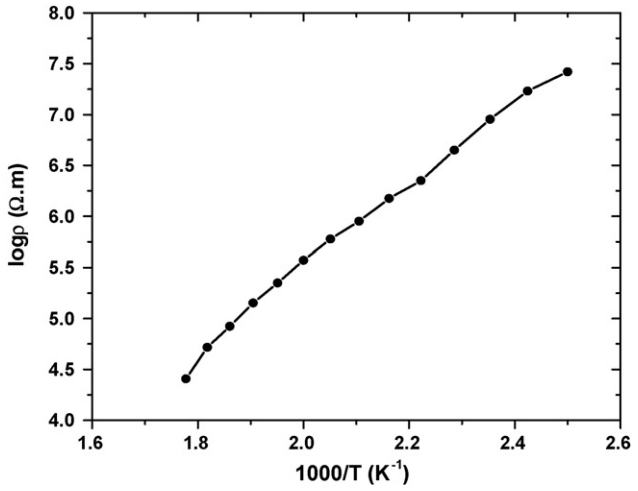

Fig. 5. Variation of dark electrical resistivity ($\log \rho$) with temperature ($1000/T$) of β-$Ni(OH)_2$.

rectangular shape. This finding suggests indicates that the capacity results mainly from a pseudo-capacitive capacitance, which is based on a redox mechanism. Redox features corresponding to anodic and cathodic peaks appear at +0.43 and +0.24 V, respectively. During the positive-going scan, the peak at +0.43 V is indicative of oxidation process while reduction takes place at +0.24 V during the negative-going scan. The appearance of anodic and cathodic peaks corresponding to the β-$Ni(OH)_2$/β-NiOOH redox reaction in the CV is according to the following electrochemical reaction:

$$\beta\text{-Ni(OH)}_2 + \text{OH}^- \rightleftarrows \beta\text{-NiOOH} + \text{H}_2\text{O} + \text{e}^- \quad \text{(D.1)}$$

The redox peaks confirm the redox behaviour of the synthesized product. The redox reaction of the nickel electrode is usually considered to be a solid-to-solid transformation [27]. Moreover, some authors [28,29] have considered that the β(II)/β(III) system follows a single-phase redox mechanism throughout the electrochemical process. The active material is thought to be a single-phase, homogeneous mixture of NiOOH and $Ni(OH)_2$, and the redox reaction involves the movement of protons and electrons into and out of the bulk of the solid phase [4].

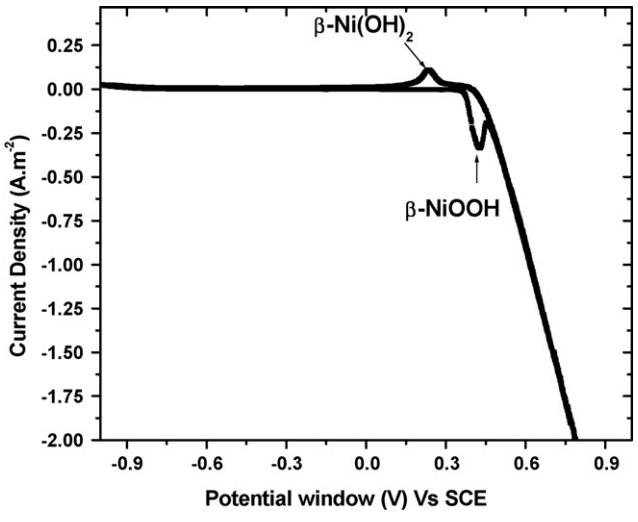

Fig. 6. Cyclic voltammogram of β-$Ni(OH)_2$ thin film electrode in 2 M KOH solution at scan rate 50 mV s^{-1} in −1 to 1 V range.

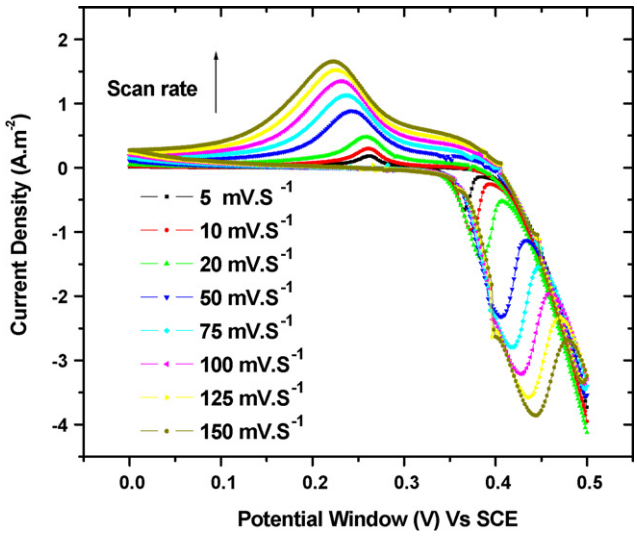

Fig. 7. Cyclic voltammograms of β-$Ni(OH)_2$ electrode at different scanning rates in 2 M KOH electrolyte in 0–0.5 V range.

3.6.1. *Effect of scan rate*

The effect of scan rate on an electrochemical supercapacitor formed by β-$Ni(OH)_2$ was studied in 2 M KOH in the voltage range of 0 to +0.5 V. The resulting CVs at different scan rates are presented in Fig. 7. The current under the curve slowly increases with scan rate. It should also be noted that as the scan rate is increased, the shape of the CV changes, the potential of the anodic and cathodic peaks shift in the more positive and negative directions, respectively, and the capacitance inevitably decreases. This shows that the voltammetric currents are directly proportional to the scan rate and thereby display capacitive behavior [30]. A plot of the specific capacitance of β-$Ni(OH)_2$ at different scan rates is shown in Fig. 8. The specific capacitance decreases from 398 to 92.42 × 10^3 F kg^{-1}, as the scan rate is increased from 5 to 150 mV s^{-1}. The decrease in capacitance is attributed to the presence of inner active sites that cannot sustain the redox transitions completely at higher scan rates. This is probably due to the diffusion effect of protons within the electrode. The decreasing capacitance suggests that parts of the surface of the electrode are inaccessible at high charging–discharging rates. Hence, the specific capacitance obtained at the slowest scan rate is believed to be closest to that of full utilization of the electrode material [31].

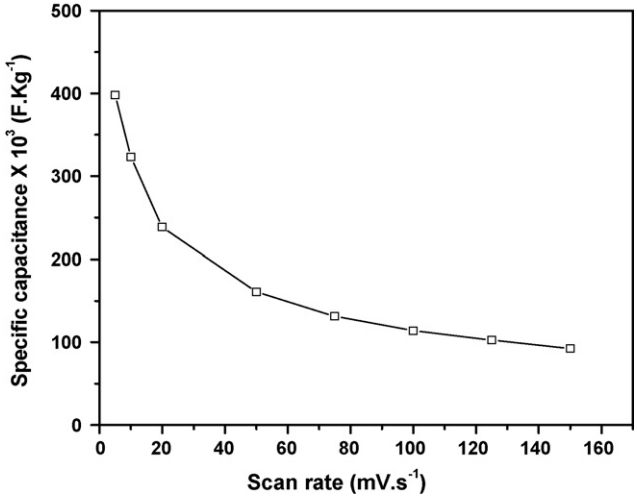

Fig. 8. Plot of specific capacitance of β-$Ni(OH)_2$ electrode at different scanning rates.

4. Conclusions

In summary, a honeycomb-like β-$Ni(OH)_2$ material has been synthesized via a facile CBD method and applied to an electrochemical capacitor. Studies with XRD, SEM, optical and electrical techniques show that β-$Ni(OH)_2$ has a less-crystallization, honeycomb-like structure with a narrow macroporous distribution, a wide optical band gap and high resistivity. The microstructure can accommodate electroactive species in the solid bulk electrode material. The specific capacitance of β-$Ni(OH)_2$ at a low scan rate is 398×10^3 F kg^{-1}, and shows a better rate capability. Thus β-$Ni(OH)_2$ is a promising electrode material for electrochemical capacitors.

Acknowledgements

One of the authors, (CDL), wishes to thank the Korean Federation of Science and Technology Societies (KOFST), for the award of Brain Pool Fellowship (2008–2009). This work was supported by the Hydrogen Energy R and D Centre, one of the 21st Century Frontier R and D programs funded by the Ministry of Science and Technology of Korea.

References

[1] P. Oliva, J. Leonardi, J.F. Laurent, C. Delmas, J.J. Braconnier, M. Figlarz, F. Fievet, J. Power Sources 8 (1982) 229.
[2] M.C. Bernard, P. Bernard, M. Keddam, S. Senyarich, H. Takenouti, Electrochem. Acta 41 (1996) 91.
[3] M. Rajamathi, G.N. Subbanna, P.V. Kamath, J. Mater. Chem. 7 (1997) 2293.
[4] S. Deabate, F. Henn, Electrochim. Acta 50 (2005) 2823.
[5] M. Fetcenko, in: D. Linden, T.B. Reddy (Eds.), Handbook of Batteries, 3rd ed., McGraw-Hill, 2001, p. 3011.
[6] P. Jeevanandam, Y. Koltypin, A. Gedanken, Nanoletters 1 (2001) 263.
[7] V. Srinivasan, J.W. Weidner, J. Electrochem. Soc. 147 (2000) 880.
[8] C. Natarajan, H. Matsumoto, G. Nogami, J. Electrochem. Soc. 144 (1997) 121.
[9] O. Baschloo, A. Hog Feldt, S.E. Lindquist, J. Phys. Chem. B 103 (1999) 8940.
[10] F.D. Mango, Org. Geochem. 24 (1996) 977.
[11] Y.E. Roginskaya, O.V. Morozova, E.N. Lubnin, Y.E. Ulitina, G.V. Lopukhova, S. Trasatti, Langmuir 13 (1997) 4621.
[12] A. Andreev, P. Khristov, A. Losev, Appl. Catal. B 7 (1996) 225.
[13] K. Watanabe, T. Kikuoka, N. Kumagai, J. Appl. Electrochem. 25 (1995) 219.
[14] X. Wang, H. Luo, P.V. Parkhutik, A. Millan, E. Matveeva, J. Power Sources (2003) 153.
[15] M. Akinc, N. Jongen, J. Lemaitre, H. Hofmann, J. Eur. Ceram. Soc. 18 (1998) 1559.
[16] M. Jayalakshmi, P. Radhika, K. Phani Raja, M. Mohan Rao, J. Solid State Electrochem. 11 (2007) 165.
[17] V. Srinivasan, J. Weidner, J. Electrochem. Soc. L120 (1997) 144.
[18] A.J. Varkey, A.F. Fort, Thin Solid Films 235 (1993) 257.
[19] B. Pejova, T. Kocareva, M. Najdoski, I. Grozdanov, Appl. Surf. Sci. 165 (2000) 271.
[20] L. Berkat, L. Cattin, A. Reguigui, C.J. Benede, Mater. Chem. Phys. 89 (2005) 11.
[21] R.S. Mane, C.D. Lokhande, Mater. Chem. Phys. 65 (2000) 1.
[22] H.M. Pathan, C.D. Lokhande, Bull. Mater. Sci. 27 (2004) 85.
[23] R.S. Patil, H.M. Pathan, T.P. Gujar, C.D. Lokhande, J. Mater. Sci. 41 (2006) 5723.
[24] Y. Li, X. Xie, J. Liu, M. Cai, J. Rogers, W. Shen, J. Chem. Eng. 136 (2008) 398.
[25] L.X. Yang, Y.J. Zhu, H. Tong, Z.H. Liang, L. Li, L. Zhang, J. Solid State Chem. 180 (2007) 2095.
[26] J. Sun, J. Cheng, C. Wang, X. Ma, M. Li, L. Yuan, Ind. Eng. Chem. Res. 5 (2006) 2146–2149.
[27] W.G. Pell, B.E. Conway, J. Electro. Chem. 500 (2001) 121.
[28] R. Barnard, C.F. Randell, F.L. Tye, J. Appl. Electrochem. 10 (1980) 109.
[29] R. Barnard, C.F. Randell, F.L. Tye, J. Appl. Electrochem. 10 (1980) 127.
[30] T.P. Gujar, V.R. Shinde, C.D. Lokhande, W.Y. Kim, K.D. Jung, O.S. Joo, Electrochem. Commun. 9 (2007) 504.
[31] T.P. Gujar, W. Kim, I. puspitasari, K.D. Jung, O.S. Joo, Int. J. Electrochem. Sci. 22 (2007) 666.